

<https://doi.org/10.15407/ujpe69.1.20>

K.T. DOVRANOV, M.T. NORMURADOV, KH.T. DAVRANOV, I.R. BEKPULATOV  
Karshi State University  
(Karshi 180100, Uzbekistan; e-mail: [qwondiqdavronm@gmail.com](mailto:qwondiqdavronm@gmail.com))

## FORMATION OF $Mn_4Si_7/Si(111)$ , $CrSi_2/Si(111)$ , AND $CoSi_2/Si(111)$ THIN FILMS AND EVALUATION OF THEIR OPTICALLY DIRECT AND INDIRECT BAND GAPS

*Now, silicon-based heterostructured nanocomposites are of great interest. Despite the fact that silicon semiconductor films (crystalline, polycrystalline, amorphous) have been systematically studied for a long time, heterostructural films are new materials, the study of which began relatively recently. We will produce and investigate the properties of heterostructured  $Mn_4Si_7/Si(111)$ ,  $CrSi_2/Si(111)$ , and  $CoSi_2/Si(111)$  thin films using infrared and ultraviolet spectroscopies. Absorption, transmission, and diffuse reflectance spectra are obtained applying FTIR spectroscopy instruments and a UV spectrophotometer. The band gap energies calculated from the transmission spectra are in the interval 0.32–1.31 eV for films deposited on the silicon substrates and in the interval 0.36–1.25 eV for the glass substrates.*

*Keywords:* FTIR spectroscopy, transmission spectroscopy, UV absorption, band gap, thin films.

### 1. Introduction

Nanoscale modifications of metal silicide films are of interest as functional materials for nanophotonics, optoelectronics, and IR detectors [1]. An important key parameter that determines the optical properties of a material is the band gap. The most common way to obtain this parameter is to use data from the absorption spectrum. However, in some cases, the direct measurement of the optical absorption is difficult due to the structural features of samples. The main purpose of this work is to implement an alternative method for determining the intervals for the band gaps of  $Mn_4Si_7/Si(111)$ ,  $CrSi_2/Si(111)$ , and  $CoSi_2/Si(111)$  thin films on the basis of the analysis of reflection spectra [2, 3].

Experimental infrared absorption measurements can be made using a dispersion-type IR spectropho-

tometer or an interference-type Fourier transform infrared (FTIR) spectrophotometer. Dispersion tools have limitations associated with low throughput and long scan times. Computerized FT-IR is very convenient, fast and allows one to get a large number of scan-averaged spectra. Commercial instruments provide a software for measuring many parameters such as peaks, subtraction spectra, etc. [4]. The effect of quantum size is manifested in this material even in crystals with a size of several tens of nanometers due to the small effective mass of the excited electron-hole pair. The quantum dots of  $Mn_4Si_7/Si(111)$ ,  $CrSi_2/Si(111)$ , and  $CoSi_2/Si(111)$  nanofilms are very attractive for mid-infrared optoelectronic devices such as photonic detectors. It is used as a target material in infrared sensors, gratings, and various optoelectronic devices [5, 6].

### 2. Literature Review

Kubelka–Munk [7] and Kumar [8] studied it on various chemical compounds and measured the band gap from infrared and ultraviolet spectra of inorganic substances.

### 3. Research Methodology

Using a molecular turbopump (Pfeiffer vacuum), a high vacuum was created in the chamber of the

Citation: Dovranov K.T., Normuradov M.T., Davranov Kh.T., Bekpulatov I.R. Formation of  $Mn_4Si_7/Si(111)$ ,  $CrSi_2/Si(111)$ , and  $CoSi_2/Si(111)$  thin film and evaluation of their optically direct and indirect band gap. *Ukr. J. Phys.* **69**, No. 1, 20 (2024). <https://doi.org/10.15407/ujpe69.1.20>.  
Цитування: Довранов К.Т., Нормурадов М.Т., Давранов Х.Т., Бекпулатов І.Р. Виготовлення тонких плівок з  $Mn_4Si_7/Si(111)$ ,  $CrSi_2/Si(111)$  та  $CoSi_2/Si(111)$  і оцінка їхніх оптично прямих та непрямих заборонених зон. *Укр. фіз. журн.* **69**, № 1, 20 (2024).

EPOS-PVD-DESK-PRO magnetron device at a pressure of  $10^{-6}$  Torr. First, the surface of the transparent glass and silicon wafers was mechanically cleaned with 25% dilute hydrofluoric acid, then the surface of the glass and silicon was re-cleaned by ionizing the argon gases inside the chamber using an “ion gun” cleaning device installed in the magnetron chamber. The current from the power source of the magnetron was 657 mA, power 240 W, voltage 320 V. Air was sucked into the chamber with the help of a turbomolecular pump until a pressure of  $10^{-5}$  Torr was reached. First, thin  $Mn_4Si_7/Si(111)$ ,  $CrSi_2/Si(111)$ , and  $CoSi_2/Si(111)$  films of various thicknesses were created at room temperature using the ion-plasma method.

The absorption, transmission, and diffuse reflection spectra were obtained using a UV-1900i spectrophotometer and the Happ–Hanzel method applying an IRTracer-100 spectrophotometer for thin films obtained by the “ion-plasma” method. One of the devices, the IRTracer-100, has the unique feature that it can be used in addition to existing accessories such as the single reflector attenuated total reflectance and diffuse reflectance devices, as well as transmission measurement accessories such as removable KBr.

In this work, the effect of substrate materials on the physical properties of deposited  $CrSi_2/Si(111)$  thin films is comprehensively studied. Two substrates are used in this study, namely, glass plates (substrate) and pure silicon wafers (substrate). As a result of the test by the ion-plasma method under high vacuum conditions, the thin layers of chromium silicide appear. The direct optical band gap of thin films is measured by extrapolating the linear portion of the square of the absorption curve to the x-axis and was developed by Kubelka–Munk. A variant of this developed method is also widely used.

#### 4. Analysis and Results

The SEM image of  $CrSi_2$  films is shown in Fig. 1. It can be seen from the figure that the individual sections of the film 90–150 nm in size (black phases) are not covered with silicon. The Si(111) surface is completely covered with an amorphous  $CrSi_2$  film with the 1-min sputtering. SEM image and RHEED pattern (inset) of a thin  $CrSi_2$  film obtained as a result of the 120-second magnetron sputtering on a silicon surface annealed at  $T = 720$  K for 1.2 h is shown in

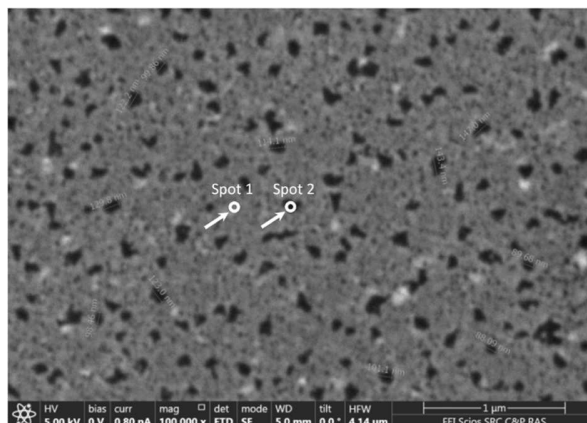


Fig. 1. SEM image of the  $CrSi_2/Si(111)$  film surface

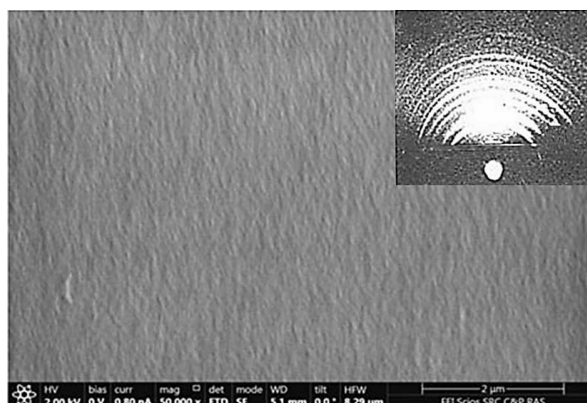


Fig. 2. SEM image and RHEED pattern (inset) of a thin  $CrSi_2$  film obtained as a result of the 120-second magnetron sputtering on a silicon surface annealed at  $T = 720$  K for 1.2 hours

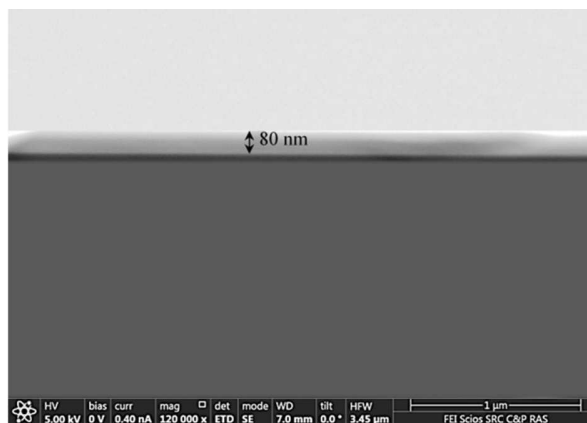


Fig. 3. SEM image of a cross-section of a thin  $CrSi_2$  film formed by the magnetron sputtering on a silicon surface for 120 s, then annealed at  $T = 720$  K for 1.2 h

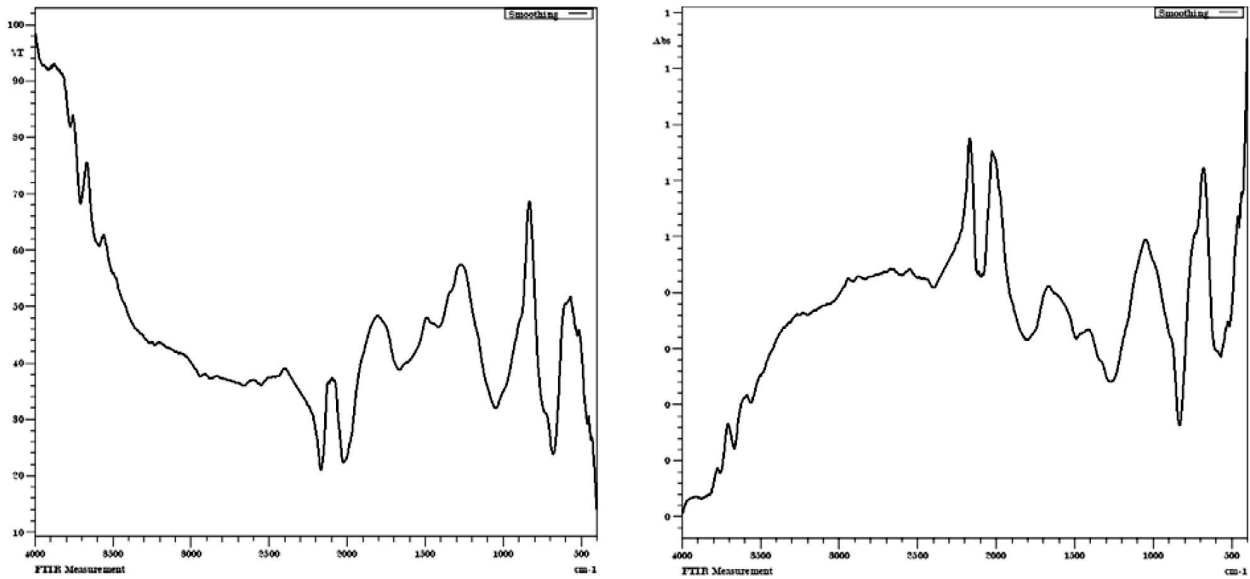


Fig. 4. Transmission and absorption spectra of chromium silicide thin films

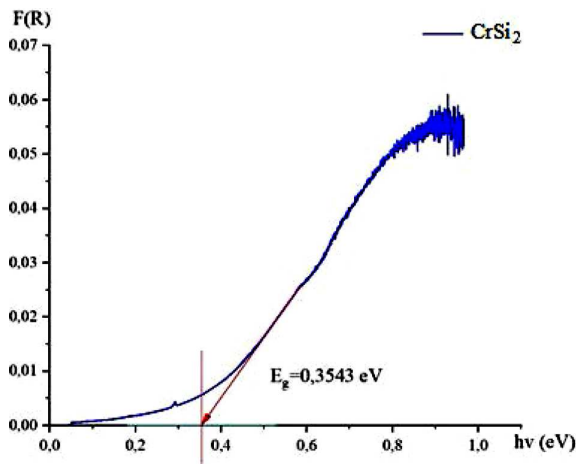


Fig. 5. Dependence of the absorption reflection function on the photon energy

Fig. 2. As can be seen from the figure, in this case, a smooth and uniform polycrystalline CrSi<sub>2</sub> film is formed. In Fig. 3, we present the SEM image of a cross-section of a thin film of the CrSi<sub>2</sub>/Si(111) system. It can be seen that the film thickness is about 80 nm.

The characteristics of diffuse reflection spectra and energy structure determine the band gap of thin films and are very important for increasing the sensitivity of optoelectronic devices and predicting their qualitative parameters. For example, the most commonly used measurement methods are thin film transmis-

sion measurements or absorption-based spectroscopic methods. These methods are preferable for measuring the optical and some electrical properties of materials, since they are mainly based on the calculation of the depth of photon penetration into the energy band gap of semiconductors [9]. Owing to the depth of penetration of photons into thin films, it is possible to determine the width of the hole or electron conduction band in them from the photon energy. When determining the optical band gap of nanoscale samples, some band width variables must be taken into account. IR spectroscopy measures parameters such as the photon energy ( $h\nu$ ), wavenumber ( $k$ ), absorption reflectance ( $F(R)$ ), and absorption and scattering coefficients ( $K, S$ ). When experimentally determining the band gap of thin films, it is a common practice to first convert the transmission spectra into pseudo-absorption spectra  $F(R)$  using the Kubelka–Munk transformation [7]:

$$F(R) = \frac{K}{S} = \frac{(1 - R)^2}{2R}. \quad (1)$$

Here,  $R$  is the reflection coefficient of the sample,  $K$  and  $S$  are the absorption and scattering coefficients, respectively. The spectra obtained by the diffuse reflection method differ from the standard transmission spectra. The spectra can be converted to Kubelka–Munk units to compensate for the differences. Fi-

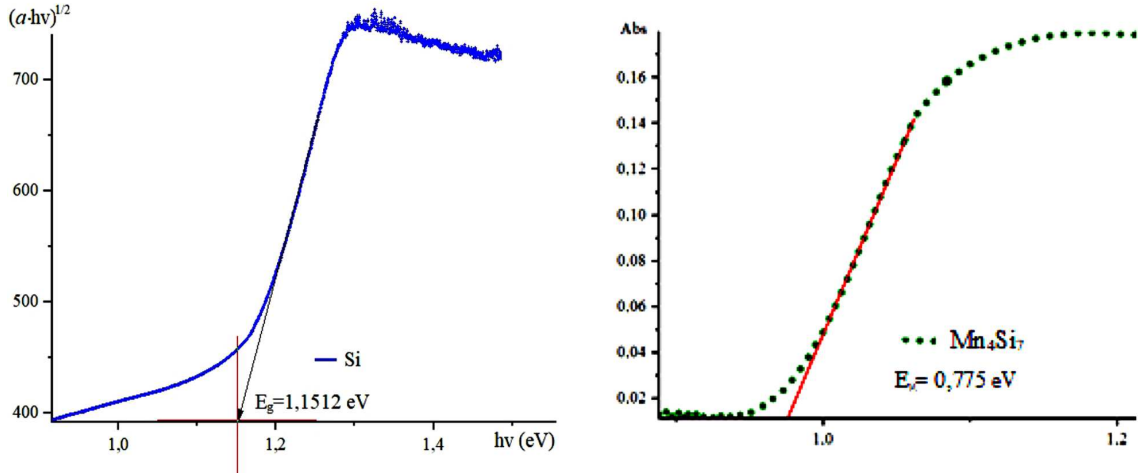


**Fig. 6.** Spectra of indirect transitions measured by the Kubelka–Munk function

figure 5 shows the band gap energy spectrum for  $CrSi_2$  calculated by the DRS method.

The scatter factor depends on both particle size and sample packaging, which explains the importance of the sample preparation for accurate results. To perform the Kubelka–Munk conversion, we select “Kubelka–Munk” from the FTIR program menu. There are no settings for this. The Kubelka–Munk equation creates a linear dependence of the spectral intensity on the sample concentration. Now, we consider the energy structure swallowing spectra and parameters.

The spectral dependences of the absorption coefficient  $\alpha(h\nu)$  were calculated using the following analytic equations and formulas recommended by Kubelka–Munk and Kumar [8]:

$$\alpha(h\nu) = \frac{\ln\left(\frac{R_{\max} - R_{\min}}{R(h\nu) - R_{\min}}\right)}{2d}. \quad (2)$$

Here,  $R_{\max}$  and  $R_{\min}$  are the maximum and minimum values, and  $d$  is the absorption layer thickness. We have

$$\alpha(h\nu) h\nu = A(h\nu - E_g)^n, \quad (3)$$

here,  $A$  is a constant,  $E_g$  are the band gaps, and  $n$  is the index determining the type of interband transitions (1/2; 3/2; 2, and 3 are directly and indirectly allowed and forbidden for transitions, respectively). Limited by information about the energy structure and nature of interband transitions in the  $CrSi_2$  film, we approximate the absorption data obtained from the

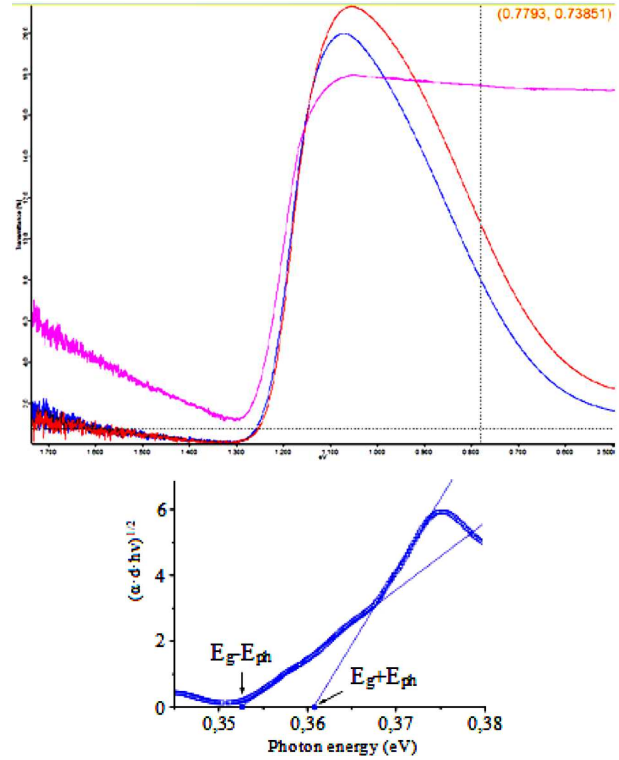


**Fig. 7.** Values of the energy gap with the absorption and emission of phonons ( $E_{ph}$ ) according to the Kumar model for manganese silicide

Kumar and Kubelka–Munk models by Eq. (3), setting the parameter  $n$  as a variable. The best fit (correlation coefficient 0.986) was achieved with values of 2 and 1/2 for  $CrSi_2$ .

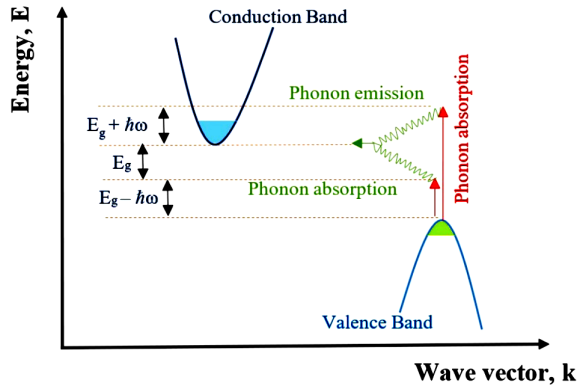


**Fig. 8.** Schematic representation of indirect interband transitions with the absorption and emission of phonons in thin films obtained by the ion-plasma method

**The obtained values of the energy gap and phonon energy for Si(111), CrSi<sub>2</sub>/Si(111), and Mn<sub>4</sub>Si<sub>7</sub>/Si(111) thin films**

Sample method	Si(111) $E_g$ , eV	CrSi <sub>2</sub> /Si(111) $E_g$ , eV	Mn <sub>4</sub> Si <sub>7</sub> /Si(111) $E_g$ , eV
Kubelka–Munk	1.1512	0.3543	0.773
Kumar model	1.132	0.362	0.684

To obtain the values of the band gap energy, we analyzed the spectral dependences of the determined absorption using the Kubelka–Munk and Kumar approaches in the coordinates of indirect optical transitions (Figs. 5 and 6).

The approximation of the linear segment in the spectral dependence of the Kubelka–Munk function by a straight line up to the intersection with the abscissa axis is equal to 1 for thin Si(111), Mn<sub>4</sub>Si<sub>7</sub>/Si(111), and CrSi<sub>2</sub>/Si(111), respectively. We get 1.512 eV, 0.773 eV, and 0.3543 eV for band gap energies for indirect transitions. More complex features are observed when using the Kumar model (Fig. 6). The absorption spectrum is characterized by two linear sections. The coordinates of the points of the intersection with the energy axis correspond to the values  $E_g + E_{ph}$  and  $E_g - E_{ph}$ , where  $E_g$  is the energy gap between the maximum and minimum conduction bands of the valence band,  $E_{ph}$  is the indirect optical energy of the involved phonons in the transition [10, 11]. In other words, there are two types of indirect transition: absorption and emission of phonons. In Fig. 7, we see a schematic representation of these transitions. The obtained values of the energy gap

and phonon energy for Si(111), CrSi<sub>2</sub>/Si(111), and Mn<sub>4</sub>Si<sub>7</sub>/Si(111) thin films are summarized in Table.

## 5. Conclusion

We have measured the band gap ( $E_g$ ) and phonon energies for heterostructured thin films obtained under high vacuum conditions by the ion-plasma method with the application of the Fourier IR and UV absorption spectroscopies. The energy gaps are determined for indirect transitions at 1.1512 eV, 0.773 eV, and 0.3543 eV for Si(111), Mn<sub>4</sub>Si<sub>7</sub>/Si(111), and CrSi<sub>2</sub>/Si(111) thin films, respectively. We have presented an approach to determining the spectral characteristics of absorption centers, types of interband transitions, and band gaps for thin films formed by the magnetron sputtering based on reflection spectra data.

1. K.C. Preetha, T.L. Remadevi. Band gap engineering in PbSe thin films from near-infrared to visible region by photochemical deposition method. *J. Mater. Sci.: Mater Electron* **25**, 1783 (2014).
2. M.T. Normuradov, Sh.T. Khozhiev, K.T. Dovranov, Kh.T. Davranov, M.A. Davlatov, F.K. Khollokov. Development of a technology for the production of nano-sized heterostructured films by ion-plasma deposition. Structure of materials. *Ukr. J. Phys.* **68** (3), (2023).
3. I.R. Bekpulatov, V.V. Loboda, M.T. Normuradov, B.D. Donaev, I.Kh. Turapov. Formation of Mn<sub>4</sub>Si<sub>7</sub> films by magnetron sputtering and a wide range of their thermoelectric properties. *St. Petersburg State Polytech. Univ. J. Physics and Mathematics* **16** (2), 78 (2023).
4. K.F. Latypov, M.Yu. Dolomatov. Estimation of the band-gap width of organic semiconductors photoconductivity by integral parameters of autocorrelational functions. *Photonics. Optoelectronic Instruments & Devices* **14** (2), 184 (2020).
5. M.T. Normuradov, Sh.T. Khozhiev, L.B. Akhmedova, I.O. Kosimov, M.A. Davlatov, K.T. Dovranov. Peculiarities of BaTiO<sub>3</sub> in electronic and X-Ray analysis. *E3S Web Conf.* **383**, 04068 (2023).
6. A. Moll, R. Viennois, M. Boehm, M. Koza, Y. Sidis. Anharmonicity and effect of the nanostructuring on the lattice dynamics of CrSi<sub>2</sub>. *J. Phys. Chem. C, American Chem. Soc.* **125** (27), 14786 (2021).
7. P. Kubelka, F. Munk. Ein beitrag zur optik der farbanstriche. *Z. Techn. Phys.* **12**, 593 (1931).
8. V. Kumar, T.P. Sharma, V. Singh. *Opt. Maitre* **12**, 115 (1999).
9. M. Wakaki, T. Shibuya, K. Kudo. *Physical Properties and Data of Optical Materials* (CRC Press Taylor Francis Group, 2007).
10. Ch. Lim, K. Park, Y. Chae, K. Kwak, M. Cho. Ultrafast continuum IR generation and its application in ir spectroscopy. *Intern. J. Mol. Sci.* **23**, 13245 (2022).

11. H.E. Kondakci, M. Yaman, A. Dana, M. Bayindir. Photonic bandgap infrared spectrometer. *Appl. Optics* **49**, 3596 (2010).

Received 12.06.23

*К.Т. Давранов, М.Т. Нормурадов,  
Х.Т. Давранов, І.Р. Бекпулатов*

ВИГОТОВЛЕННЯ ТОНКИХ ПЛІВОК  
З  $Mn_4Si_7/Si(111)$ ,  $CrSi_2/Si(111)$  ТА  $CoSi_2/Si(111)$   
І ОЦІНКА ЇХНІХ ОПТИЧНО ПРЯМИХ  
ТА НЕПРЯМИХ ЗАБОРОНЕНИХ ЗОН

Виготовлено тонкі плівки з  $Mn_4Si_7/Si(111)$ ,  $CrSi_2/Si(111)$   
та  $CoSi_2/Si(111)$  з неоднорідною структурою і дослідже-

но їх властивості методами спектроскопії інфрачервоного і ультрафіолетового світла. Із застосуванням інфрачервоної Фур'є-спектроскопії отримано спектри поглинання, трансмісійні та дифузійного відбиття. Використовуючи трансмісійні спектри, розраховано, що енергії заборонених зон належать інтервалу 0,32–1,31 еВ для плівок на кремнії і 0,36–1,25 еВ для плівок на склі.

*Ключові слова:* інфрачервоної Фур'є-спектроскопія, трансмісійна спектроскопія, поглинання ультрафіолетового світла, заборонена зона, тонкі плівки.